

# CHAPTER 18

## FAILURE CONSIDERATIONS

**Jack Collins**

Department of Mechanical Engineering  
Ohio State University  
Columbus, Ohio

**Steve Daniewicz**

Department of Mechanical Engineering  
Mississippi State University  
Starkville, Mississippi

<b>18.1</b>	<b>CRITERIA OF FAILURE</b>	<b>377</b>			
<b>18.2</b>	<b>FAILURE MODES</b>	<b>378</b>			
<b>18.3</b>	<b>ELASTIC DEFORMATION AND YIELDING</b>	<b>382</b>			
<b>18.4</b>	<b>FRACTURE MECHANICS AND UNSTABLE CRACK GROWTH</b>	<b>383</b>			
<b>18.5</b>	<b>FATIGUE AND STRESS CONCENTRATION</b>	<b>396</b>			
18.5.1	Fatigue Loading and Laboratory Testing	397			
18.5.2	The <i>S-N-P</i> Curves—A Basic Design Tool	401			
18.5.3	Factors That Affect <i>S-N-P</i> Curves	402			
18.5.4	Nonzero Mean and Multiaxial Fatigue Stresses	402			
18.5.5	Spectrum Loading and Cumulative Damage	410			
18.5.6	Stress Concentration	414			
18.5.7	Low-Cycle Fatigue	420			
18.5.8	Three-Phase Approach for Fatigue Life Prediction	429			
18.5.9	Service Spectrum Simulation and Full-Scale Testing	435			
18.5.10	Damage Tolerance and Fracture Control	436			
<b>18.6</b>	<b>CREEP AND STRESS RUPTURE</b>	<b>437</b>			
18.6.1	Prediction of Long-Term Creep Behavior	439			
18.6.2	Creep under Uniaxial State of Stress	440			
18.6.3	Creep under Multiaxial State of Stress	442			
18.6.4	Cumulative Creep	442			
<b>18.7</b>	<b>COMBINED CREEP AND FATIGUE</b>	<b>443</b>			
<b>18.8</b>	<b>FRETTING AND WEAR</b>	<b>449</b>			
18.8.1	Fretting Phenomena	450			
18.8.2	Wear Phenomena	456			
<b>18.9</b>	<b>CORROSION AND STRESS CORROSION</b>	<b>462</b>			
18.9.1	Types of Corrosion	463			
18.9.2	Stress Corrosion Cracking	467			
<b>18.10</b>	<b>FAILURE ANALYSIS AND RETROSPECTIVE DESIGN</b>	<b>468</b>			

### 18.1 CRITERIA OF FAILURE

Any change in the size, shape, or material properties of a structure, machine, or machine part that renders it incapable of performing its intended function must be regarded as a mechanical failure of the device. It should be carefully noted that the key concept here is that *improper functioning* of a machine part constitutes failure. Thus, a shear pin that does *not* separate into two or more pieces upon the application of a preselected overload must be regarded as having failed as surely as a drive shaft has failed if it *does* separate into two pieces under normal expected operating loads.

Failure of a device or structure to function properly might be brought about by any one or a combination of many different responses to loads and environments while in service. For example, too much or too little elastic deformation might produce failure. A fractured load-carrying structural member or a shear pin that does not shear under overload conditions each would constitute failure. Progression of a crack due to fluctuating loads or aggressive environment might lead to failure after a period of time if resulting excessive deflection or fracture interferes with proper machine function.

A primary responsibility of any mechanical designer is to ensure that his or her design functions as intended for the prescribed design lifetime and, at the same time, that it be competitive in the marketplace. Success in designing competitive products while averting premature mechanical failures can be achieved consistently only by recognizing and evaluating all potential modes of failure that might govern the design. To recognize potential failure modes a designer must be acquainted with the array of failure modes observed in practice, and with the conditions leading to these failures. The following section summarizes the mechanical failure modes most commonly observed in practice, followed by a brief description of each one.

## 18.2 FAILURE MODES

A failure mode may be defined as the physical process or processes that take place or that combine their effects to produce a failure, as just discussed. In the following list of commonly observed failure modes it may be noted that some failure modes are unilateral phenomena, whereas others are combined phenomena. For example, fatigue is listed as a failure mode, corrosion is listed as a failure mode, and corrosion fatigue is listed as still another failure mode. Such combinations are included because they are commonly observed, important, and often *synergistic*. In the case of corrosion fatigue, for example, the presence of active corrosion aggravates the fatigue process and at the same time the presence of a fluctuating load accelerates the corrosion process.

The following list is not presented in any special order but it includes all commonly observed modes of mechanical failure:<sup>1</sup>

1. Force and/or temperature-induced elastic deformation.
2. Yielding.
3. Brinnelling.
4. Ductile rupture.
5. Brittle fracture.
6. Fatigue:
  - a. High-cycle fatigue
  - b. Low-cycle fatigue
  - c. Thermal fatigue
  - d. Surface fatigue
  - e. Impact fatigue
  - f. Corrosion fatigue
  - g. Fretting fatigue
7. Corrosion:
  - a. Direct chemical attack
  - b. Galvanic corrosion
  - c. Crevice corrosion
  - d. Pitting corrosion
  - e. Intergranular corrosion
  - f. Selective leaching
  - g. Erosion corrosion
  - h. Cavitation corrosion
  - i. Hydrogen damage
  - j. Biological corrosion
  - k. Stress corrosion
8. Wear:
  - a. Adhesive wear
  - b. Abrasive wear
  - c. Corrosive wear
  - d. Surface fatigue wear
  - e. Deformation wear
  - f. Impact wear

- g. Fretting wear
- 9. Impact:
  - a. Impact fracture
  - b. Impact deformation
  - c. Impact wear
  - d. Impact fretting
  - e. Impact fatigue
- 10. Fretting:
  - a. Fretting fatigue
  - b. Fretting wear
  - c. Fretting corrosion
- 11. Creep.
- 12. Thermal relaxation.
- 13. Stress rupture.
- 14. Thermal shock.
- 15. Galling and seizure.
- 16. Spalling.
- 17. Radiation damage.
- 18. Buckling.
- 19. Creep buckling.
- 20. Stress corrosion.
- 21. Corrosion wear.
- 22. Corrosion fatigue.
- 23. Combined creep and fatigue.

As commonly used in engineering practice, the failure modes just listed may be defined and described briefly as follows. It should be emphasized that these failure modes only produce failure when they generate a set of circumstances that interferes with the proper functioning of a machine or device.

*Force and/or temperature-induced elastic deformation* failure occurs whenever the elastic (recoverable) deformation in a machine member, brought about by the imposed operational loads or temperatures, becomes large enough to interfere with the ability of the machine to perform its intended function satisfactorily.

*Yielding* failure occurs when the plastic (unrecoverable) deformation in a ductile machine member, brought about by the imposed operational loads or motions, becomes large enough to interfere with the ability of the machine to perform its intended function satisfactorily.

*Brinelling* failure occurs when the static forces between two curved surfaces in contact result in local yielding of one or both mating members to produce a permanent surface discontinuity of significant size. For example, if a ball bearing is statically loaded so that a ball is forced to indent permanently the race through local plastic flow, the race is brinnelled. Subsequent operation of the bearing might result in intolerably increased vibration, noise, and heating; and, therefore, failure would have occurred.

*Ductile rupture* failure occurs when the plastic deformation, in a machine part that exhibits ductile behavior, is carried to the extreme so that the member separates into two pieces. Initiation and coalescence of internal voids slowly propagate to failure, leaving a dull, fibrous rupture surface.

*Brittle fracture* failure occurs when the elastic deformation, in a machine part that exhibits brittle behavior, is carried to the extreme so that the primary interatomic bonds are broken and the member separates into two or more pieces. Preexisting flaws or growing cracks form initiation sites for very rapid crack propagation to catastrophic failure, leaving a granular, multifaceted fracture surface.

*Fatigue* failure is a general term given to the sudden and catastrophic separation of a machine part into two or more pieces as a result of the application of fluctuating loads or deformations over a period of time. Failure takes place by the initiation and propagation of a crack until it becomes unstable and propagates suddenly to failure. The loads and deformations that typically cause failure by fatigue are far below the static failure levels. When loads or deformations are of such magnitude that more than about 10,000 cycles are required to produce failure, the phenomenon is usually termed *high-cycle fatigue*. When loads or deformations are of such magnitude that less than about 10,000 cycles are required to produce failure, the phenomenon is usually termed *low-cycle fatigue*. When load or strain cycling is produced by a fluctuating temperature field in the machine part, the process is usually termed *thermal fatigue*. *Surface fatigue* failure, usually associated with rolling surfaces in contact, manifests itself as pitting, cracking, and spalling of the contacting surfaces as a result of the cyclic Hertz contact stresses that result in maximum values of cyclic shear stresses slightly below

the surface. The cyclic subsurface shear stresses generate cracks that propagate to the contacting surface, dislodging particles in the process to produce surface pitting. This phenomenon is often viewed as a type of wear. Impact fatigue, corrosion fatigue, and fretting fatigue are described later.

*Corrosion* failure, a very broad term, implies that a machine part is rendered incapable of performing its intended function because of the undesired deterioration of the material as a result of chemical or electrochemical interaction with the environment. Corrosion often interacts with other failure modes such as wear or fatigue. The many forms of corrosion include the following. *Direct chemical attack*, perhaps the most common type of corrosion, involves corrosive attack of the surface of the machine part exposed to the corrosive media, more or less uniformly over the entire exposed surface. *Galvanic corrosion* is an accelerated electrochemical corrosion that occurs when two dissimilar metals in electrical contact are made part of a circuit completed by a connecting pool or film of electrolyte or corrosive medium, leading to current flow and ensuing corrosion. *Crevice corrosion* is the accelerated corrosion process highly localized within crevices, cracks, or joints where small volume regions of stagnant solution are trapped in contact with the corroding metal. *Pitting corrosion* is a very localized attack that leads to the development of an array of holes or pits that penetrate the metal. *Intergranular corrosion* is the localized attack occurring at grain boundaries of certain copper, chromium, nickel, aluminum, magnesium, and zinc alloys when they are improperly heat treated or welded. Formation of local galvanic cells that precipitate corrosion products at the grain boundaries seriously degrades the material strength because of the intergranular corrosive process. *Selective leaching* is a corrosion process in which one element of a solid alloy is removed, such as in dezincification of brass alloys or graphitization of gray cast irons. *Erosion corrosion* is the accelerated chemical attack that results when abrasive or viscid material flows past a containing surface, continuously baring fresh, unprotected material to the corrosive medium. *Cavitation corrosion* is the accelerated chemical corrosion that results when, because of differences in vapor pressure, certain bubbles and cavities within a fluid collapse adjacent to the pressure-vessel walls, causing particles of the surface to be expelled, baring fresh, unprotected surface to the corrosive medium. *Hydrogen damage*, while not considered to be a form of direct corrosion, is induced by corrosion. Hydrogen damage includes hydrogen blistering, hydrogen embrittlement, hydrogen attack, and decarburization. *Biological corrosion* is a corrosion process that results from the activity of living organisms, usually by virtue of their processes of food ingestion and waste elimination, in which the waste products are corrosive acids or hydroxides. *Stress corrosion*, an extremely important type of corrosion, is described separately later.

*Wear* is the undesired cumulative change in dimensions brought about by the gradual removal of discrete particles from contacting surfaces in motion, usually sliding, predominantly as a result of mechanical action. Wear is not a single process, but a number of different processes that can take place by themselves or in combination, resulting in material removal from contacting surfaces through a complex combination of local shearing, plowing, gouging, welding, tearing, and others. *Adhesive wear* takes place because of high local pressure and welding at asperity contact sites, followed by motion-induced plastic deformation and rupture of asperity functions, with resulting metal removal or transfer. *Abrasive wear* takes place when the wear particles are removed from the surface by the plowing, gouging, and cutting action of the asperities of a harder mating surface or by hard particles entrapped between the mating surfaces. When the conditions for either adhesive wear or abrasive wear coexist with conditions that lead to corrosion, the processes interact synergistically to produce *corrosive wear*. As described earlier, *surface fatigue wear* is a wear phenomenon associated with curved surfaces in rolling or sliding contact, in which subsurface cyclic shear stresses initiate microcracks that propagate to the surface to spall out macroscopic particles and form wear pits. *Deformation wear* arises as a result of repeated *plastic* deformation at the wearing surfaces, producing a matrix of cracks that grow and coalesce to form wear particles. Deformation wear is often caused by severe impact loading. *Impact wear* is impact-induced repeated *elastic* deformation at the wearing surface that produces a matrix of cracks that grows in accordance with the surface fatigue description just given. Fretting wear is described later.

*Impact failure* results when a machine member is subjected to nonstatic loads that produce in the part stresses or deformations of such magnitude that the member no longer is capable of performing its function. The failure is brought about by the interaction of stress or strain waves generated by dynamic or suddenly applied loads, which may induce local stresses and strains many times greater than would be induced by the static application of the same loads. If the magnitudes of the stresses and strains are sufficiently high to cause separation into two or more parts, the failure is called *impact fracture*. If the impact produces intolerable elastic or plastic deformation, the resulting failure is called *impact deformation*. If repeated impacts induce cyclic elastic strains that lead to initiation of a matrix of fatigue cracks, which grows to failure by the surface fatigue phenomenon described earlier, the process is called *impact wear*. If fretting action, as described in the next paragraph, is induced by the small lateral relative displacements between two surfaces as they impact together, where the small displacements are caused by Poisson strains or small tangential "glancing" velocity components, the phenomenon is called *impact fretting*. *Impact fatigue* failure occurs when impact

loading is applied repetitively to a machine member until failure occurs by the nucleation and propagation of a fatigue crack.

*Fretting* action may occur at the interface between any two solid bodies whenever they are pressed together by a normal force and subjected to small-amplitude cyclic relative motion with respect to each other. Fretting usually takes place in joints that are not intended to move but, because of vibrational loads or deformations, experience minute cyclic relative motions. Typically, debris produced by fretting action is trapped between the surfaces because of the small motions involved. *Fretting fatigue* failure is the premature fatigue fracture of a machine member subjected to fluctuating loads or strains together with conditions that simultaneously produce fretting action. The surface discontinuities and microcracks generated by the fretting action act as fatigue crack nuclei that propagate to failure under conditions of fatigue loading that would otherwise be acceptable. Fretting fatigue failure is an insidious failure mode because the fretting action is usually hidden within a joint where it cannot be seen and leads to premature, or even unexpected, fatigue failure of a sudden and catastrophic nature. *Fretting wear* failure results when the changes in dimensions of the mating parts, because of the presence of fretting action, become large enough to interfere with proper design function or large enough to produce geometrical stress concentration of such magnitude that failure ensues as a result of excessive local stress levels. *Fretting corrosion* failure occurs when a machine part is rendered incapable of performing its intended function because of the surface degradation of the material from which the part is made, as a result of fretting action.

*Creep* failure results whenever the plastic deformation in a machine member accrues over a period of time under the influence of stress and temperature until the accumulated dimensional changes interfere with the ability of the machine part to perform satisfactorily its intended function. Three stages of creep are often observed: (1) transient or primary creep during which time the rate of strain decreases, (2) steady-state or secondary creep during which time the rate of strain is virtually constant, and (3) tertiary creep during which time the creep strain rate increases, often rapidly, until rupture occurs. This terminal rupture is often called creep rupture and may or may not occur, depending on the stress–time–temperature conditions.

*Thermal relaxation* failure occurs when the dimensional changes due to the creep process result in the relaxation of a prestrained or prestressed member until it no longer is able to perform its intended function. For example, if the prestressed flange bolts of a high-temperature pressure vessel relax over a period of time because of creep in the bolts, so that, finally, the peak pressure surges exceed the bolt preload to violate the flange seal, the bolts will have failed because of thermal relaxation.

*Stress rupture* failure is intimately related to the creep process except that the combination of stress, time, and temperature is such that rupture into two parts is ensured. In stress rupture failures the combination of stress and temperature is often such that the period of steady-state creep is short or nonexistent.

*Thermal shock* failure occurs when the thermal gradients generated in a machine part are so pronounced that differential thermal strains exceed the ability of the material to sustain them without yielding or fracture.

*Galling* failure occurs when two sliding surfaces are subjected to such a combination of loads, sliding velocities, temperatures, environments, and lubricants that massive surface destruction is caused by welding and tearing, plowing, gouging, significant plastic deformation of surface asperities, and metal transfer between the two surfaces. Galling may be thought of as a severe extension of the adhesive wear process. When such action results in significant impairment to intended surface sliding or in seizure, the joint is said to have failed by galling. *Seizure* is an extension of the galling process to such severity that the two parts are virtually welded together so that relative motion is no longer possible.

*Spalling* failure occurs whenever a particle is spontaneously dislodged from the surface of a machine part so as to prevent the proper function of the member. Armor plate fails by spalling, for example, when a striking missile on the exposed side of an armor shield generates a stress wave that propagates across the plate in such a way as to dislodge or spall a secondary missile of lethal potential on the protected side. Another example of spalling failure is manifested in rolling contact bearings and gear teeth because of the action of surface fatigue as described earlier.

*Radiation damage* failure occurs when the changes in material properties induced by exposure to a nuclear radiation field are of such a type and magnitude that the machine part is no longer able to perform its intended function, usually as a result of the triggering of some other failure mode, and often related to loss in ductility associated with radiation exposure. Elastomers and polymers are typically more susceptible to radiation damage than are metals, whose strength properties are sometimes enhanced rather than damaged by exposure to a radiation field, although ductility is usually decreased.

*Buckling* failure occurs when, because of a critical combination of magnitude and/or point of load application, together with the geometrical configuration of a machine member, the deflection of the member suddenly increases greatly with only a slight change in load. This nonlinear response

results in a buckling failure if the buckled member is no longer capable of performing its design function.

*Creep buckling* failure occurs when, after a period of time, the creep process results in an unstable combination of the loading and geometry of a machine part so that the critical buckling limit is exceeded and failure ensues.

*Stress corrosion* failure occurs when the applied stresses on a machine part in a corrosive environment generate a field of localized surface cracks, usually along grain boundaries, that render the part incapable of performing its function, often because of triggering some other failure mode. Stress corrosion is a very important type of corrosion failure mode because so many different metals are susceptible to it. For example, a variety of iron, steel, stainless-steel, copper, and aluminum alloys are subject to stress corrosion cracking if placed in certain adverse corrosive media.

*Corrosion wear* failure is a combination failure mode in which corrosion and wear combine their deleterious effects to incapacitate a machine part. The corrosion process often produces a hard, abrasive corrosion product that accelerates the wear, while the wear process constantly removes the protective corrosion layer from the surface, baring fresh metal to the corrosive medium and thus accelerating the corrosion. The two modes combine to make the result more serious than either of the modes would have been otherwise.

*Corrosion fatigue* is a combination failure mode in which corrosion and fatigue combine their deleterious effects to cause failure of a machine part. The corrosion process often forms pits and surface discontinuities that act as stress raisers which in turn accelerate fatigue failure. Furthermore, cracks in the usually brittle corrosion layer also act as fatigue crack nuclei that propagate into the base material. On the other hand, the cyclic loads or strains cause cracking and flaking of the corrosion layer, which bares fresh metal to the corrosive medium. Thus, each process accelerates the other, often making the result disproportionately serious.

*Combined creep and fatigue* failure is a combination failure mode in which all of the conditions for both creep failure and fatigue exist simultaneously, each process influencing the other to produce failure. The interaction of creep and fatigue is probably synergistic but is not well understood.

### 18.3 ELASTIC DEFORMATION AND YIELDING

Small changes in the interatomic spacing of a material, brought about by applied forces or changing temperatures, are manifested macroscopically as elastic strain. Although the maximum elastic strain in crystalline solids, including engineering metals, is typically very small, the force required to produce the small strain is usually large; hence, the accompanying stress is large. On the other hand, certain other noncrystalline materials such as elastomers may exhibit recoverable (but not necessarily linear) strains of several hundred percent. For uniaxial loading of a machine or structural element, the total elastic deformation of the member may be found by integrating the elastic strain over the length of the element. Thus, for a uniform bar subjected to uniaxial loading the total deformation of the bar in the axial direction is

$$\Delta l = l\epsilon \quad (18.1)$$

where  $\Delta l$  is total axial deformation of the bar,  $l$  is the original bar length, and  $\epsilon$  is the axial elastic strain. If  $\Delta l$  exceeds the design-allowable axial deformation, failure will occur. For example, if the axial deformation of an aircraft gas-turbine blade, due to the centrifugal force field, exceeds the tip clearance gap, failure will occur because of force-induced elastic deformation. Likewise, if thermal expansion of the blade produces a blade-axial deformation that exceeds the tip clearance gap, failure will occur because of temperature-induced elastic deformation.

When the state of stress is more complicated, it becomes necessary to calculate the elastic strains induced by the multiaxial states of stress in three mutually perpendicular directions through the use of the generalized Hooke's law equations given by

$$\begin{aligned} \epsilon_x &= \frac{1}{E} [\sigma_x - \nu(\sigma_y + \sigma_z)] \\ \epsilon_y &= \frac{1}{E} [\sigma_y - \nu(\sigma_x + \sigma_z)] \\ \epsilon_z &= \frac{1}{E} [\sigma_z - \nu(\sigma_x + \sigma_y)] \end{aligned} \quad (18.2)$$

where  $\sigma_x$ ,  $\sigma_y$ , and  $\sigma_z$  are the normal stresses in the three coordinate directions,  $E$  and  $\nu$  are Young's modulus and Poisson's ratio, respectively, and  $\epsilon_x$ ,  $\epsilon_y$ , and  $\epsilon_z$  are the elastic strains in the three coordinate directions. Again, total elastic deformation of a member in any of the coordinate directions may be found by integrating the strain over the member's length in that direction. If the change in length of the member in any direction exceeds the design-allowable deformation in that direction, failure will occur. The use of commercial finite element analysis software packages is one commonly

used means of determining both the elastic strains produced in a structural element and the subsequent elastic deformations produced.

If applied loads reach certain critical levels, the atoms within the microstructure may be moved into new equilibrium positions and the induced strains are not fully recovered upon release of the loads. Such permanent strains, usually the result of slip, are called plastic strains, and the macroscopic permanent deformation due to plastic strain is called yielding. If applied loads are increased even more, the plastic deformation process may be carried to the point of instability where *necking* begins: internal voids form and slowly coalesce to finally produce a ductile rupture of the loaded member.

After plastic deformation has been initiated, the Hooke's law equations (18.2) are no longer valid and the predictions of plastic strains and deformations under multiaxial states of stress are more difficult. If a designer can tolerate a prescribed plastic deformation without experiencing failure, these plastic deformations may be determined using plasticity theory. Many commercial finite element analysis software packages now possess the capability to compute both plastic strains and deformations for a prescribed nonlinear elastic-plastic constitutive relation.

For the case of simple uniaxial loading, the onset of yielding may be accurately predicted to occur when the uniaxial maximum normal stress reaches a value equal to the yield point strength of the material read from an engineering stress-strain curve. If the loading is more complicated, and a multiaxial state of stress is produced by the loads, the onset of yielding may no longer be predicted by comparing any one of the normal stress components with uniaxial material yield strength, not even the maximum principal normal stress. Onset of yielding for multiaxially stressed critical points in a machine or structure is more accurately predicted through the use of a *combined stress theory of failure*, which has experimentally been validated for the prediction of yielding. The two most widely accepted theories for predicting the onset of yielding are the distortion energy theory (also called the octahedral shear stress theory or the Huber-von Mises-Hencky theory) and the maximum shearing stress theory. The distortion energy theory is somewhat more accurate while the maximum shearing stress theory may be slightly easier to use.

In words, the distortion energy theory may be expressed as follows:

*Failure is predicted to occur in the multiaxial state of stress when the distortion energy per unit volume becomes equal to or exceeds the distortion energy per unit volume at the time of failure in a simple uniaxial stress test using a specimen of the same material.*

Mathematically, the distortion energy theory may be formulated as

*Failure is predicted by the distortion energy theory to occur if*

$$\frac{1}{2}[(\sigma_1 - \sigma_2)^2 + (\sigma_2 - \sigma_3)^2 + (\sigma_3 - \sigma_1)^2] \geq \sigma_f^2 \quad (18.3)$$

The maximum shearing stress theory may be stated in words as:

*Failure is predicted to occur in the multiaxial state of stress when the maximum shearing stress magnitude becomes equal to or exceeds the maximum shearing stress magnitude at the time of failure in a simple uniaxial stress test using a specimen of the same material.*

Mathematically, the maximum shearing stress theory becomes:

*Failure is predicted by the maximum shearing stress theory to occur if*

$$\sigma_1 - \sigma_3 \geq \sigma_f \quad (18.4)$$

where  $\sigma_1$ ,  $\sigma_2$ , and  $\sigma_3$  are the principal stresses at a point, ordered such that  $\sigma_1 \geq \sigma_2 \geq \sigma_3$ , and  $\sigma_f$  is the uniaxial failure strength in tension.

Comparisons of these two failure theories with experimental data on yielding are shown in Fig. 18.1 for a variety of materials and different biaxial states of stress.

## 18.4 FRACTURE MECHANICS AND UNSTABLE CRACK GROWTH

When the material behavior is brittle rather than ductile, the mechanics of the failure process are much different. Instead of the slow coalescence of voids associated with ductile rupture, brittle fracture proceeds by the high-velocity propagation of a crack across the loaded member. If the material behavior is clearly brittle, fracture may be predicted with reasonable accuracy through use of the maximum normal stress theory of failure. In words, the maximum normal stress theory may be expressed as follows:

*Failure is predicted to occur in the multiaxial state of stress when the maximum principal normal stress becomes equal to or exceeds the maximum normal stress at the time of failure in a simple uniaxial stress test using a specimen of the same material.*

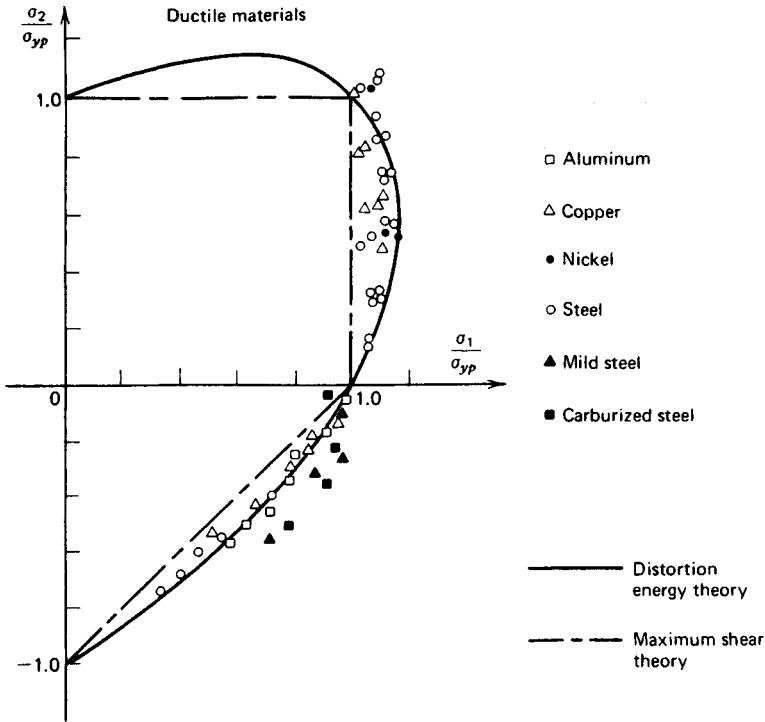


**Fig. 18.1** Comparison of biaxial yield strength data with theories of failure for a variety of ductile materials.

Mathematically, the maximum normal stress theory becomes:

*Failure is predicted by the maximum normal stress theory to occur if*

$$\sigma_1 > \sigma_t \quad \sigma_3 \leq \sigma_c \quad (18.5)$$

where  $\sigma_1$ ,  $\sigma_2$ , and  $\sigma_3$  are the principal stresses at a point, ordered such that  $\sigma_1 \geq \sigma_2 \geq \sigma_3$ ,  $\sigma_t$  is the uniaxial failure strength in tension, and  $\sigma_c$  is the uniaxial failure strength in compression. Comparison of this failure theory with experimental data on brittle fracture for different biaxial states of stress is shown in Fig. 18.2.

On the other hand, more recent experience has led to the understanding that nominally ductile materials may also fail by a brittle fracture response in the presence of cracks or flaws if the combination of crack size, geometry of the part, temperature, and/or loading rate lies within certain critical regions. Furthermore, the development of higher-strength structural alloys, the wider use of welding, and the use of thicker sections in some cases have combined their influence to reduce toward a critical level the capacity of some structural members to accommodate local plastic strain without fracture. At the same time, fabrication by welding, residual stresses due to machining, and assembly mismatch in production have increased the need for accommodating local plastic strain to prevent failure. Fluctuating service loads of greater severity and more aggressive environments have also contributed to unexpected fractures. From the study of all these factors the basic concepts of *fracture control* were conceived and developed. Fracture control consists, simply, of controlling the nominal stress and crack size so that the combination always lies below a critical level for the material being used in a given design application.

An important observation in studying fracture behavior is that the magnitude of the nominal applied stress that causes fracture is related to the size of the crack or cracklike flaw within the structure.<sup>2</sup> For example, observations of the behavior of central through-the-thickness cracks, oriented normal to the applied tensile stress, in steel and aluminum plates, yielded the results shown in Figs. 18.3 and 18.4. In these tests, as the tensile loading on the precracked plates was slowly increased, the crack extension slowly increased for a time and then abruptly extended to failure by rapid crack

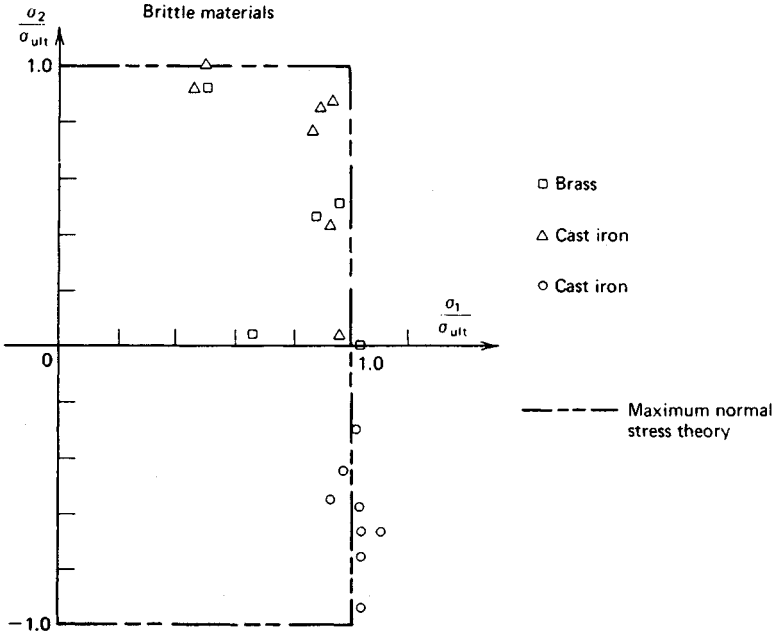


**Fig. 18.2** Comparison of biaxial brittle fracture strength data with maximum normal stress theory for several brittle materials.

propagation. Slow stable crack growth was characterized by speeds of the order of fractions of an inch per minute. Rapid crack propagation was characterized by speeds of the order of hundreds of feet per second. The data of Figs. 18.3 and 18.4 indicate that for longer initial crack length the fracture stress, that is, the stress corresponding to the onset of rapid crack extension, was lower. For the aluminum alloy the fracture stress was less than the yield strength for cracks longer than about 0.75 in. For the steel alloy the fracture stress was less than the yield strength for cracks longer than about 0.5 in. In both cases, for shorter cracks the fracture stress approaches the ultimate strength of the material determined from a conventional uniaxial tension test.

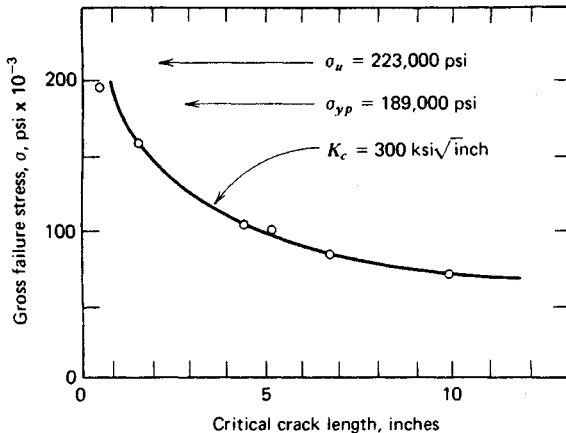


**Fig. 18.3** Influence of crack length on gross failure stress for center cracked steel plate, 36 in. wide, 0.14 in. thick, room temperature, 4330 M steel, longitudinal direction. (After Ref. 2, copyright ASTM: adapted with permission.)

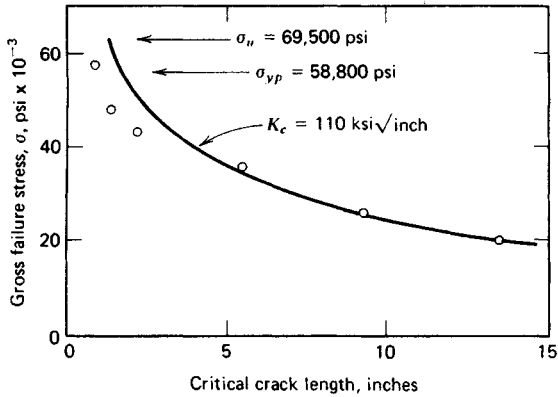


**Fig. 18.4** Influence of crack length on gross failure stress for center cracked aluminum plate, 24 in. wide, 0.1 in. thick, room temperature, 2219-T87 aluminum alloy, longitudinal direction. (After Ref. 2, copyright ASTM, adapted with permission.)

Experience has shown that the abrupt change from slow crack growth to rapid unstable crack growth establishes an important material property termed *fracture toughness*. The fracture toughness may be used as a design criterion in fracture prevention, just as the yield strength is used as a design criterion in prevention of yielding of a ductile material under static loading.

In many cases slow crack propagation is also of interest, especially under conditions of fluctuating loads and/or aggressive environments. In analyses and predictions involving fatigue failure phenomena, characterization of the rate of slow crack extension and the initial flaw size, together with critical crack size, are used to determine the useful life of a component or structure subjected to fluctuating loads. The topic of fatigue crack propagation is discussed further in Section 18.5.

The simplest useful model for stress at the tip of a crack is based on the assumptions of linear elastic material behavior and a two-dimensional analysis; thus, the procedure is often referred to as linear elastic fracture mechanics. Although the validity of the linear elastic assumption may be questioned in view of plastic zone formation at the tip of a crack in any real engineering material, as long as "small-scale yielding" occurs, that is, as long as the plastic zone size remains small compared to the dimensions of the crack, the linear elastic model gives good engineering results. Thus, the small-scale yielding concept implies that the small plastic zone is confined within a linear elastic field surrounding the crack tip. If the material properties, section size, loading conditions, and environment combine in such a way that "large-scale" plastic zones are formed, the basic assumptions of linear elastic fracture mechanics are violated, and elastic-plastic fracture mechanics methods must be employed.

Three basic types of stress fields can be defined for crack-tip stress analysis, each one associated with a distinct mode of crack deformation, as illustrated in Fig. 18.5. The opening mode, mode I, is associated with local displacement in which the crack surfaces move directly apart, as shown in Fig. 18.5a. The sliding mode, mode II, is developed when crack surfaces slide over each other in a direction perpendicular to the leading edge of the crack, as shown in Fig. 18.5b. The tearing mode, mode III, is characterized by crack surfaces sliding with respect to each other in a direction parallel to the leading edge of the crack, as shown in Fig. 18.5c. Superposition of these three modes will fully describe the most general three-dimensional case of local crack-tip deformation and stress field, although mode I is most common.

Based on the methods developed by Westergaard,<sup>3</sup> Irwin<sup>4</sup> developed the two-dimensional stress field and displacement field equations for each of the three modes depicted in Fig. 18.5, expressing them in terms of the coordinates shown in Fig. 18.6.

For mode I, the stress components in the crack-tip stress field are

$$\sigma_x = \frac{K_I}{\sqrt{2\pi r}} \cos \frac{\theta}{2} \left[ 1 - \sin \frac{\theta}{2} \sin \frac{3\theta}{2} \right] + \sigma_{x_0} + [O]r^{1/2} \quad (18.6)$$

$$\sigma_y = \frac{K_I}{\sqrt{2\pi r}} \cos \frac{\theta}{2} \left[ 1 + \sin \frac{\theta}{2} \sin \frac{3\theta}{2} \right] + [O]r^{1/2} \quad (18.7)$$

$$\tau_{xy} = \frac{K_I}{\sqrt{2\pi r}} \sin \frac{\theta}{2} \cos \frac{\theta}{2} \cos \frac{3\theta}{2} + [O]r^{1/2} \quad (18.8)$$

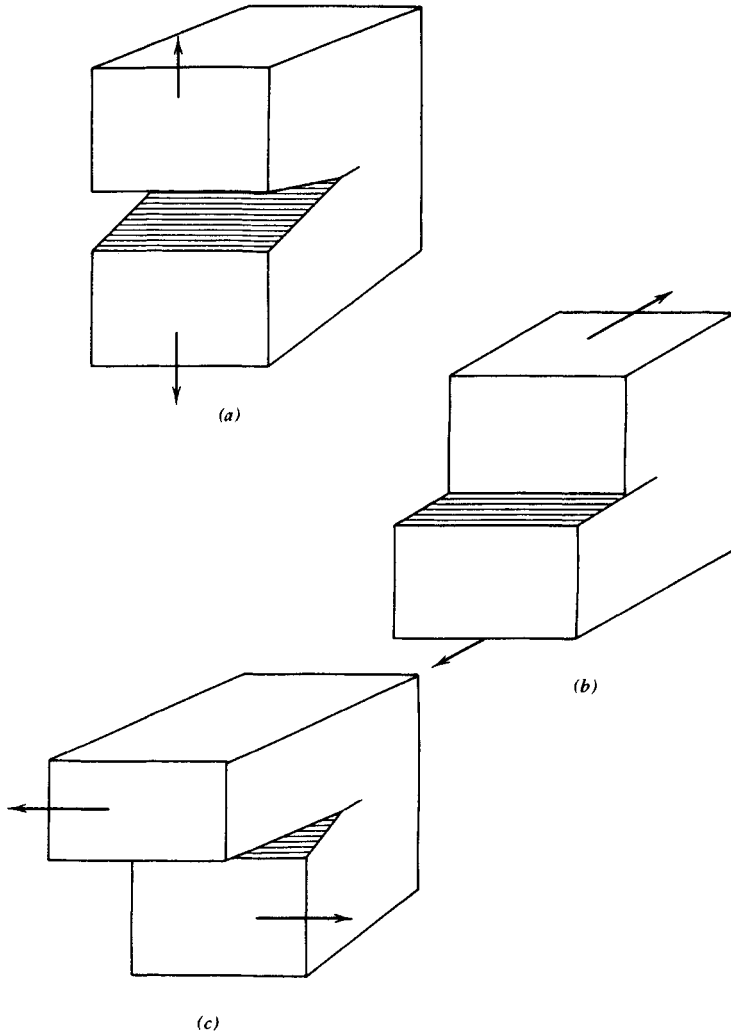


**Fig. 18.5** Basic modes of crack displacement: (a) mode I; (b) model II; (c) mode III.

For conditions of plane strain, where displacements in the  $z$  direction are constrained to be zero (thick members), the remaining three stress components are

$$\sigma_z = \nu(\sigma_x + \sigma_y) \quad (18.9)$$

$$\tau_{xz} = 0 \quad (18.10)$$

$$\tau_{yz} = 0 \quad (18.11)$$

For mode II, the stress components in the crack-tip stress field are

$$\sigma_x = \frac{-K_{II}}{\sqrt{2\pi r}} \sin \frac{\theta}{2} \left[ 2 + \cos \frac{\theta}{2} \cos \frac{3\theta}{2} \right] + \sigma_{x_0} + [O]r^{1/2} \quad (18.12)$$

$$\sigma_y = \frac{K_{II}}{\sqrt{2\pi r}} \sin \frac{\theta}{2} \cos \frac{\theta}{2} \cos \frac{3\theta}{2} + [O]r^{1/2} \quad (18.13)$$

$$\tau_{xy} = \frac{K_{II}}{\sqrt{2\pi r}} \cos \frac{\theta}{2} \left[ 1 - \sin \frac{\theta}{2} \sin \frac{3\theta}{2} \right] + [O]r^{1/2} \quad (18.14)$$

and, for plane strain conditions,

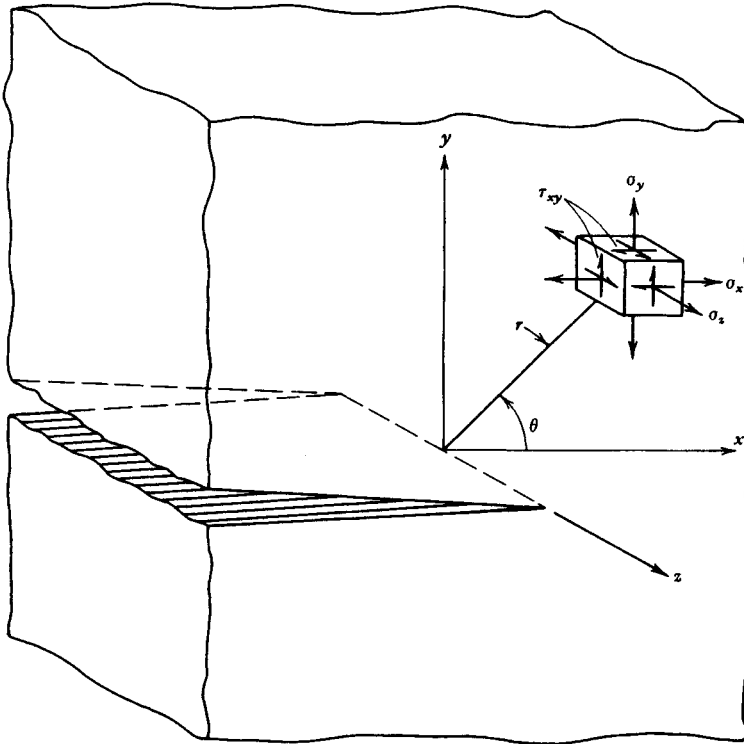


Fig. 18.6 Coordinates measured from leading edge of a crack.

$$\sigma_z = \nu(\sigma_x + \sigma_y) \quad (18.15)$$

$$\tau_{xy} = 0 \quad (18.16)$$

$$\tau_{yz} = 0 \quad (18.17)$$

For mode III, the stress components in the crack-tip stress field are

$$\tau_{xz} = \frac{-K_{III}}{\sqrt{2\pi r}} \sin \frac{\theta}{2} + \tau_{xz0} + [O]r^{1/2} \quad (18.18)$$

$$\tau_{yz} = \frac{K_{III}}{\sqrt{2\pi r}} \cos \frac{\theta}{2} + [O]r^{1/2} \quad (18.19)$$

$$\sigma_x = \sigma_y = \sigma_z = \tau_{xy} = 0 \quad (18.20)$$

In expressions (18.6) through (18.20), higher-order terms such as the uniform stresses parallel to cracks  $\sigma_{x0}$  and  $\tau_{xz0}$ , and terms of the order of  $r^{1/2}$ , that is,  $[O]r^{1/2}$ , are indicated. These terms are usually neglected as higher order compared to the leading  $1/\sqrt{r}$  term. The parameters  $K_I$ ,  $K_{II}$ , and  $K_{III}$  are called crack-tip stress field intensity factors, or simply *stress intensity factors*. They represent the *strength* of the stress field surrounding the tip of the crack. Physically,  $K_I$ ,  $K_{II}$ , and  $K_{III}$  may be interpreted as the intensity of load transmittal through the crack-tip region, induced by the introduction of a crack into a flaw-free body. Since fracture is induced by the crack-tip stress field, the stress intensity factors are primary correlation parameters in current practice.

For remote loadings, in general, the expressions for the stress intensity factor are of the form

$$K = C\sigma\sqrt{\pi a} \quad (18.21)$$

where  $C$  is dependent on the type of loading and the geometry away from the crack. Much work has been completed in determining values of  $C$  for a wide variety of conditions. (See, for example, Ref. 5.)

Many commercial finite element analysis software packages possess special crack tip elements allowing the numerical computation of stress intensity factors. A discussion of some of the techniques employed within these software packages is given by Anderson.<sup>6</sup> Through the use of weight functions,<sup>7</sup> stress intensity factors may be computed using numerical integration. This analysis technique is ideally suited for use with personal computers and will be discussed in more detail in the following paragraphs.

For a given cracked plate, for example, Fig. 18.6, the factor  $K$  increases proportionally with gross nominal stress and also is a function of the instantaneous crack length. Thus,  $K$  is a single-parameter measure of the stress field around the crack tip. The value of  $K$  associated with the onset of rapid crack extension has been designated the *critical stress intensity*,  $K_c$ . As noted earlier in Figs. 18.3 and 18.4, the onset of rapid crack propagation for specimens with different initial crack lengths occurs at different values of gross-section stress, but at a constant value of  $K_c$ . Thus,  $K_c$  provides a single-parameter fracture criterion that allows the prediction of fracture based on (18.21). That is, *fracture is predicted to occur if*

$$C\sigma\sqrt{\pi a} \geq K_c \quad (18.22)$$

In studying material behavior, one finds that for a given material, depending on the state of stress at the crack tip, the critical stress intensity  $K_c$  decreases to a lower limiting value as the state of strain approaches the condition of plane strain. This lower limiting value defines a basic material property  $K_{Ic}$ , the *plane strain fracture toughness* for the material. Standard test methods have been established for the determination of  $K_{Ic}$  values.<sup>8</sup> A few data are shown in Table 18.1. Useful compilations of fracture toughness values have been prepared by several organizations and individuals. These include Refs. 10–16.

For the plane strain fracture toughness  $K_{Ic}$  to be a valid failure prediction criterion for a specimen or a machine part, plane strain conditions must exist at the crack tip; that is, the material must be *thick* enough to ensure plane strain conditions. It has been estimated empirically that for plane strain conditions the minimum material thickness  $B$  must be

$$B \geq 2.5 \left( \frac{K_{Ic}}{\sigma_{yp}} \right)^2 \quad (18.23)$$

where  $\sigma_{yp}$  is the material yield strength.

If the material is not thick enough to meet the criterion of (18.23), plane stress is a more likely state of stress at the crack tip; and  $K_c$ , the critical stress intensity factor for failure prediction under plane stress conditions, may be estimated using a semi-empirical relationship for  $K_c$ .<sup>17,18</sup>

$$K_c = K_{Ic} \left[ 1 + \frac{1.4}{B^2} \left( \frac{K_{Ic}}{\sigma_{yp}} \right)^4 \right]^{1/2} \quad (18.24)$$

As long as the crack-tip plastic zone remains in the regime of small-scale yielding, this estimation

**Table 18.1 Yield Strength and Plane Strain Fracture Toughness Data for Selected Engineering Alloys<sup>9,10</sup>**

Alloy	Form	Test Temperature		$\sigma_{yp}$		$K_{Ic}$	
		°F	°C	ksi	MPa	ksi√in	MPa√m
4340 (500°F temper) steel	Plate	70	21	217–238	1495–1640	45–57	50–63
4340 (800°F temper) steel	Forged	70	21	197–211	1360–1455	72–83	79–91
D6AC (1000°F temper) steel	Plate	70	21	217	1495	93	102
D6AC (1000°F temper) steel	Plate	–65	–54	228	1570	56	62
A 538 steel				250	1722	100	111
2014-T6 aluminum	Forged	75	24	64	440	28	31
2024-T351 aluminum	Plate	80	27	54–56	370–385	28–40	31–44
7075-T6 aluminum				85	585	30	33
7075-T651 aluminum	Plate	70	21	75–81	515–560	25–28	27–31
7075-T7351 aluminum	Plate	70	21	58–66	400–455	28–32	31–35
Ti-6Al-4V titanium	Plate	74	23	119	820	96	106

procedure provides a good design approach. For conditions that result in large crack-tip plastic zones (large applied stresses, large crack lengths), performing a failure assessment using linear elastic fracture mechanics (LEFM) is invalid and potentially nonconservative. A general rule of thumb is that plasticity effects become significant when the applied stresses approach 50% of the yield stress, but this is by no means a universal rule.<sup>6</sup> When small-scale yielding is not generated at the crack tip, a better design approach would involve the implementation of an appropriate elastic-plastic fracture mechanics procedure, such as a *failure assessment diagram* (FAD). This methodology will be discussed in more detail in the following paragraphs.

A more useful estimate defining the limits of LEFM applicability may be formulated using the fracture toughness test specimen size requirements set forth by the ASTM.<sup>8</sup> For a valid plane strain fracture toughness test, one implying that LEFM is valid, the crack size  $a$  must satisfy  $a > 2.5 (K_{IC}/\sigma_{yp})^2$ . From Eq. (18.7), with  $\theta = 0$ , the stress  $\sigma_y$  will equal the yield stress  $\sigma_{yp}$  when

$$r_y = \alpha \left( \frac{K_I}{\sigma_{yp}} \right)^2 \quad (18.25)$$

where  $\alpha = 1/2\pi$ . This equation is an initial estimate of the plastic zone size in a nonhardening material under plane stress conditions. For plane strain conditions  $\alpha = 1/6\pi$ .<sup>19</sup> A subsequent force balance may be used to show that a more reasonable estimate is  $2r_y$ .<sup>19</sup> However, strain hardening effects will reduce the size of the plastic zone; consequently Eq. (18.25) may be considered a first order estimate of the actual plastic zone size.

With  $\alpha = 1/6\pi$  and  $K_I = K_{IC}$ , Eq. (18.25) gives the maximum possible plastic zone size under plane strain conditions. Substituting this result into the ASTM crack size requirement gives  $a > 50 r_y$  (approximately). Defining the distance  $d$  as the smallest in-plane dimension from the crack tip to the nearest free surface as shown in Fig. 18.7, this result suggests that, in general, small-scale yielding conditions may be expected if<sup>6</sup>

$$r_y < d/50 \quad (18.26)$$

where  $r_y$  is the maximum plastic zone size, computed from Eq. (18.25) with  $\alpha = 1/6\pi$ ,  $K_I = K_{IC}$  for plane strain and  $\alpha = 1/2\pi$ ,  $K_I = K_C$  for plane stress.

In predicting failure for designing a part so that failure will not occur, a designer must, at an early stage, identify the probable mode of failure, employ a suitable "modulus" by which severity of loading and environment may be represented analytically, select a material and geometry for the proposed part, and obtain pertinent critical material strength properties related to the probable failure mode. He must next calculate the magnitude of the selected "modulus" under applicable loading and environmental conditions and compare the calculated magnitude of the modulus with the proper critical material strength property. Failure is predicted to occur if the magnitude of the selected modulus equals or exceeds the critical material strength parameter.

For example, if a designer determines yielding to be a potential failure mode for his or her part, he or she would probably select stress ( $\sigma$ ) as his or her "modulus" and the uniaxial yield point strength ( $\sigma_{yp}$ ) as the critical material strength parameter. The designer would then assess the quality of his or her design by asserting that *failure is predicted to occur if*

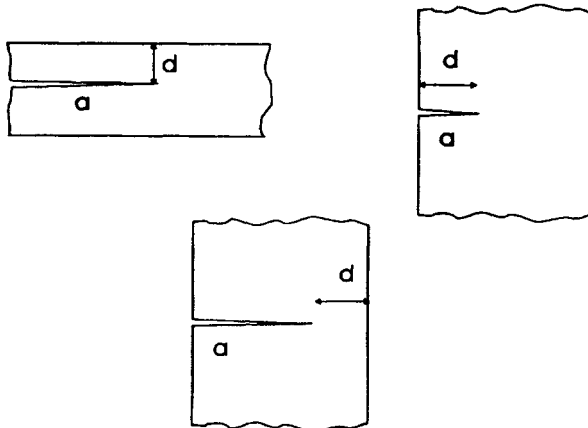


Fig. 18.7 Smallest in-plane distance  $d$  from crack tip to nearest free surface.

$$\sigma \geq \sigma_{sp} \quad (18.27)$$

The fracture mechanics approach is useful to the designer in precisely the same way when brittle fracture is a possible failure mode. The designer would select stress intensity factor  $K$  as his or her "modulus" and fracture toughness  $K_c$  as the appropriate critical strength parameter and assert that failure is predicted to occur if

$$K \geq K_c \quad (18.28)$$

Although the details of calculating  $K$  and determining  $K_c$  for some cases may be difficult, the basic concept of predicting failure by brittle fracture is no more complicated than this. It is worth noting that in most cases a designer would be well advised to consider both the possibility of failure by brittle fracture and also the possibility of failure by yielding.

To utilize (18.28) as a design or failure prediction tool, the stress intensity factor must be determined for the particular loading and geometry of the part or structure under investigation. To illustrate the procedure, several configurations are mentioned here, with many more solutions available in the literature. (See, for example, Refs. 5, 20, and 21.)

For *central through-the-thickness cracks* and *single edge through-the-thickness cracks* under *direct tension loading* or *shear loading*, the form of the stress intensity factor is

$$K = C\sigma_t\sqrt{\pi a} \quad (18.29)$$

or

$$K = C\tau\sqrt{\pi a} \quad (18.30)$$

where  $C$  is a function of geometry and crack displacement mode, as given in Figs. 18.8 and 18.9.

For a *beam* with a *single through-the-thickness edge crack* under a *pure bending moment*, the form of the stress intensity factor is

$$K_1 = C_1\sigma_b\sqrt{\pi a} \quad (18.31)$$

where  $C_1$  is a function of geometry, as given in Fig. 18.10, and the gross section bending stress  $\sigma_b$  is

$$\sigma_b = \frac{6M}{tb^2} \quad (18.32)$$

For a *through-the-thickness crack emanating from a circular hole* in an infinite plate under *biaxial tension*, the form of the stress intensity factor is

$$K_1 = C_1\sigma\sqrt{\pi a} \quad (18.33)$$

where  $C_1$  is a function of geometry and the ratio of biaxial stress components, as shown in Fig. 18.11.

For a *part-through thumbnail surface crack* in a plate subjected to *uniform tension loading*, the form of the stress intensity factor is

$$K_1 = \frac{1.12}{\sqrt{Q}}\sigma_t\sqrt{\pi a} \quad (18.34)$$

where  $Q$  is a surface flaw shape parameter that depends on the ratio of crack depth to length and the ratio of nominal applied stress to yield strength of the material, as shown in Fig. 18.12.

Stress intensity factors may also be determined using weight functions.<sup>6,7,23</sup> Generally, this technique involves the use of numerical integration. It is ideally suited for use with personal computers. The primary advantage of the weight function technique is its capability to consider arbitrary applied stress distributions, as opposed to the pure bending or uniform tension stress distributions illustrated in Figs. 18.8, 18.9, 18.10, and 18.11.

Weight functions are unique for a given cracked geometry, with many weight functions available in the literature (see, for example, Refs. 7 and 23). Given the weight function  $m(x, a)$  for a given geometry exhibiting a through-thickness crack of length  $a$ , and the applied stress distribution  $\sigma(x)$  along the crack line  $x$  in the uncracked body, the stress intensity factor may be written

$$K_I(a) = \int_0^a \sigma(x)m(x, a) dx \quad (18.35)$$

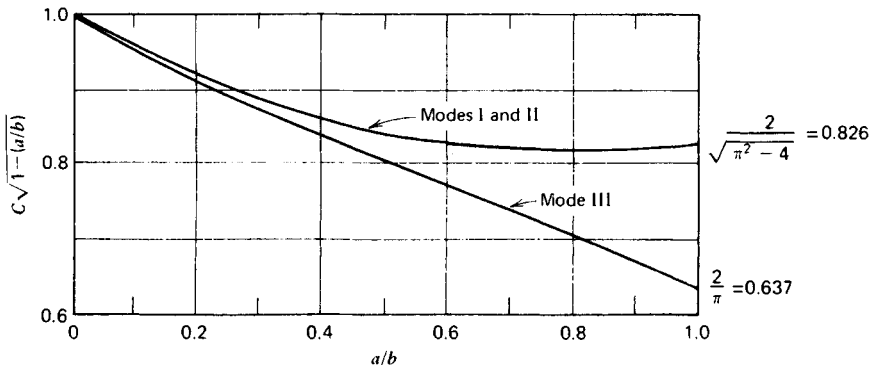
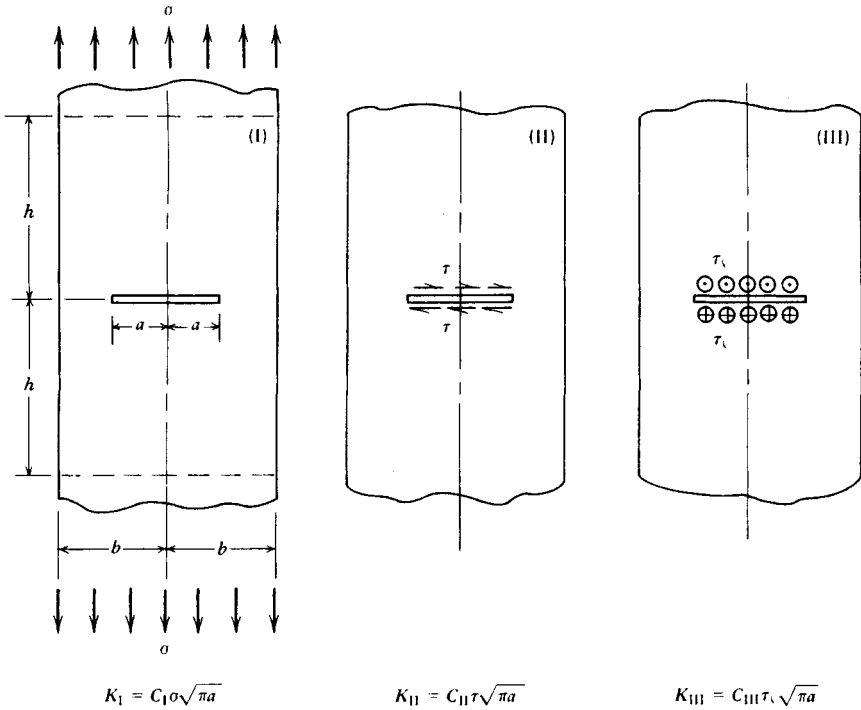


**Fig. 18.8** Stress intensity factors  $K_I$ ,  $K_{II}$ , and  $K_{III}$  for center cracked test specimen. (From Ref. 5, copyright Del Research Corp.; adapted with permission.)

For a single through-thickness crack of length  $a$  in a strip with width  $b$  (see Fig. 18.9), an approximate weight function is given by<sup>23</sup>

$$m(x, a) = \sqrt{\frac{2}{\pi(a-x)}} \left[ 1 + m_1 \left( 1 - \frac{x}{a} \right) + m_2 \left( 1 - \frac{x}{a} \right)^2 \right] \quad (18.36)$$

where  $m_1$  and  $m_2$  are functions of the crack length to width ratio ( $a/b$ ). For  $0 \leq a/b \leq 1/2$

$$\begin{aligned} m_1 &= A_1 + B_1(a/b)^2 + C_1(a/b)^6 \\ m_2 &= A_2 + B_2(a/b)^2 + C_2(a/b)^6 \end{aligned} \quad (18.37)$$

$A_1 = 0.6147, B_1 = 17.1844, C_1 = 8.7822$   
 $A_2 = 0.2502, B_2 = 3.2899, C_2 = 70.0444$

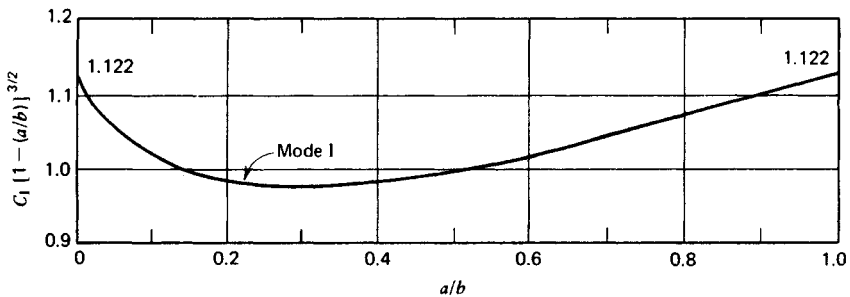
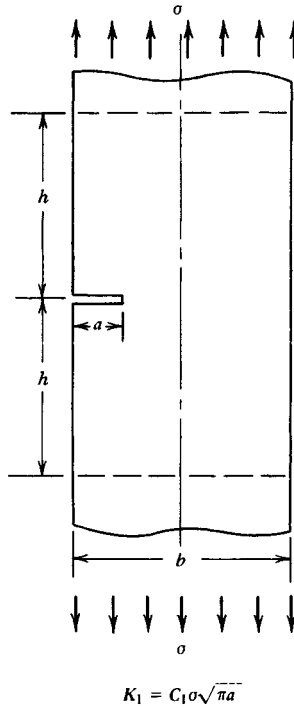
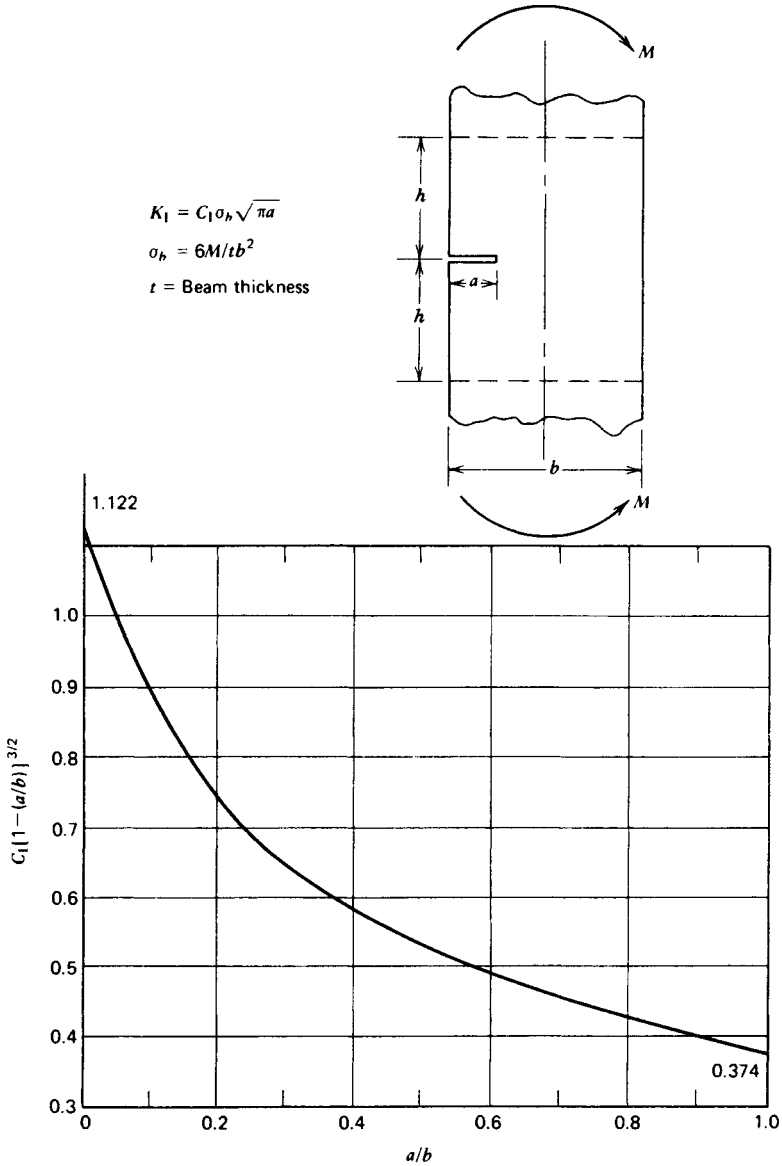


Fig. 18.9 Stress intensity factor  $K_I$  for single edge notch test specimen. (From Ref. 5, copyright Del Research Corp.; reprinted with permission.)

This weight function, in conjunction with Eq. (18.35), may be used to compute stress intensity factors for arbitrary applied stress distributions  $\sigma(x)$  determined through an analysis of the uncracked body.

Using the stress intensity factor, together with fracture toughness properties for the material of interest, a designer may utilize (18.28) to predict failure or, more important, to design a part so that failure will not occur under service loading. It should be reiterated that fracture toughness is not only a function of metallurgical factors such as alloy composition and heat treatment, but a function of service temperature, loading rate, and state of stress in the vicinity of the crack tip as well. In many practical applications the plastic zone size ahead of the crack tip becomes so large that the assumption of small-scale yielding is no longer valid, and elastic analyses using the stress intensity factor are no longer appropriate. When small-scale yielding conditions are not satisfied, a better design approach would be to implement an appropriate elastic-plastic fracture mechanics (EPFM) methodology. One such methodology involves the use of a *failure assessment diagram* (FAD).<sup>6,18,24</sup>

Under small-scale yielding conditions, fracture under predominantly elastic conditions is predicted to occur when the stress intensity factor equals or exceeds the material fracture toughness. Alternately, failure by plastic collapse may occur if the plastic zone becomes sufficiently large such that it



**Fig. 18.10** Stress intensity factor  $K_I$  for single through-the-thickness edge crack under pure bending moment. (From Ref. 5, copyright Del Research Corp.; adapted with permission.)

encompasses the entire remaining ligament ahead of the crack. Plastic collapse is predicted to occur when the applied stress equals the plastic collapse stress  $\sigma_c$ . This applied stress corresponds to a stress in the uncracked ligament equal to the yield stress. Under intermediate conditions, in which the crack tip plastic zone does not encompass the entire remaining ligament and yet is not small, an interaction between elastic fracture and plastic collapse defines the governing failure mode. The FAD allows an approximate assessment of this interaction.

Defining  $K_r = K_I/K_c$  and  $S_r = \sigma/\sigma_c$ , where  $\sigma$  is the stress used to compute  $K_I$ , failure is predicted to occur when

$$K_r = S_r \left\{ \frac{8}{\pi^2} \ln \left[ \sec \left( \frac{\pi}{2} S_r \right) \right] \right\}^{-1/2} \quad (18.38)$$

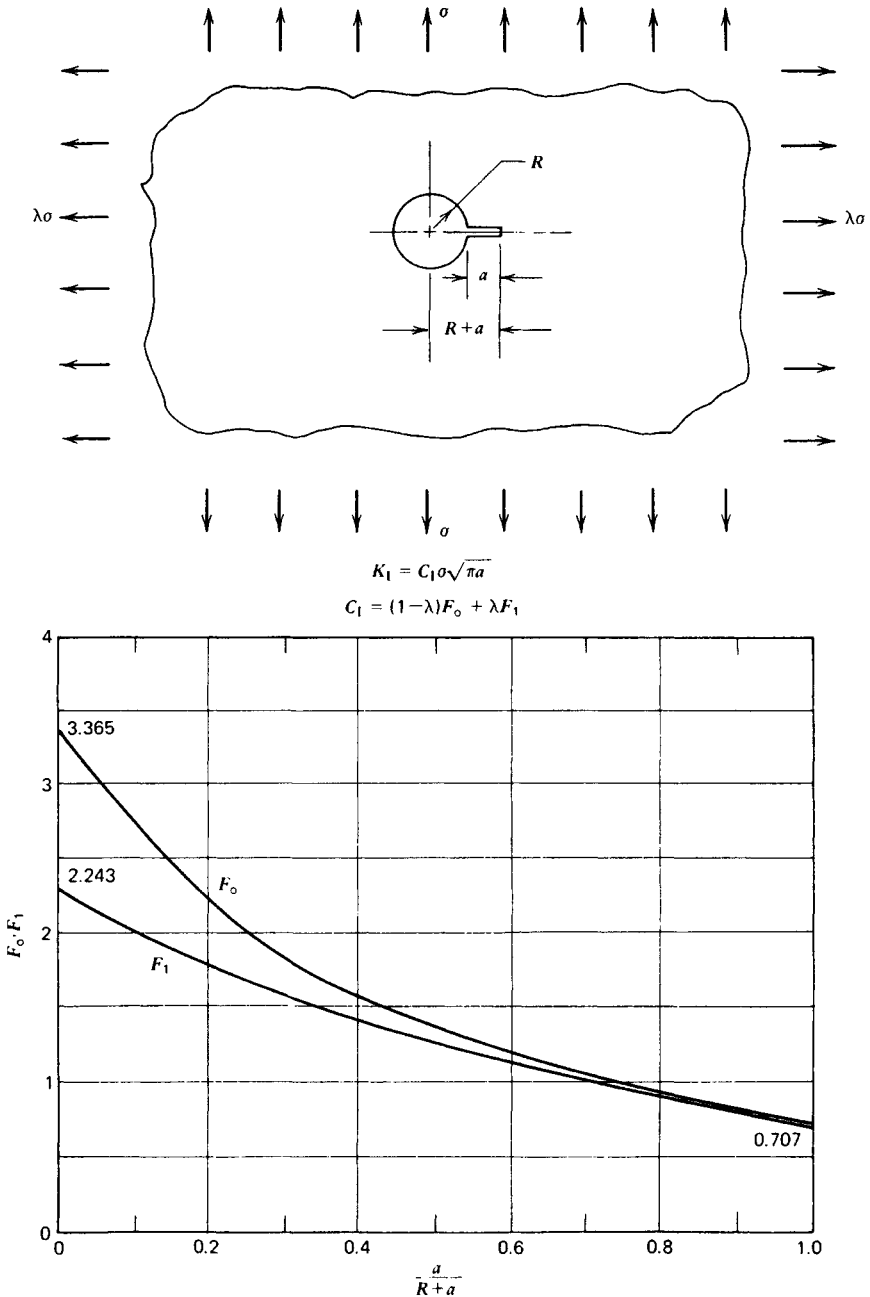


**Fig. 18.11** Stress intensity factor  $K_I$  for a through-the-thickness crack emanating from a circular hole in an infinite plate under biaxial tension. (From Ref. 5, copyright Del Research Corp.; adapted with permission.)

Equation (18.38) represents a failure curve in the  $K_r$ - $S_r$  plane. This curve is illustrated in Fig. 18.13 and is known as the failure assessment diagram or the R6 curve. The integrity of a flawed structure may be assessed by computing  $S_r$  and  $K_r$  and plotting this point on the FAD. For a point falling within the curve, no failure is predicted. For points falling on or outside the curve, failure is predicted to occur.

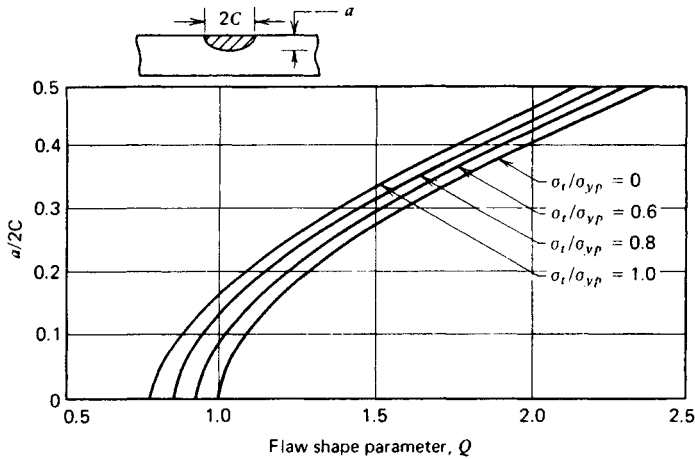


**Fig. 18.12** Surface flaw shape parameter. (From Ref. 22. Adapted by permission of Prentice-Hall, Inc., Englewood Cliffs, New Jersey.)

To approximate the effects of strain hardening, a flow stress  $\sigma_o$ , taken to be an average of the yield and ultimate strengths, is often used when computing the plastic collapse stress. The plastic collapse stress  $\sigma_c$  is that applied stress which produces  $\sigma_o$  across the remaining uncracked ligament, and is the maximum applied stress that a perfectly plastic material can sustain. This stress may be determined using a limit load analysis. In general, the plastic collapse stress is a function of geometry, type of loading, type of support (boundary conditions), and through-thickness constraint (plane stress or plane strain).<sup>6,25</sup> For a single through-thickness crack of length  $a$  in a strip with width  $b$  loaded in tension (see Fig. 18.9), if end rotations are restrained, the plastic collapse stress under plane stress conditions may be approximated by<sup>25</sup>

$$\sigma_c = \sigma_o(1 - a/b) \tag{18.39}$$

**18.5 FATIGUE AND STRESS CONCENTRATION**

Static or quasistatic loading is rarely observed in modern engineering practice, making it essential for the designer to address himself or herself to the implications of repeated loads, fluctuating loads, and rapidly applied loads. By far, the majority of engineering design projects involve machine parts

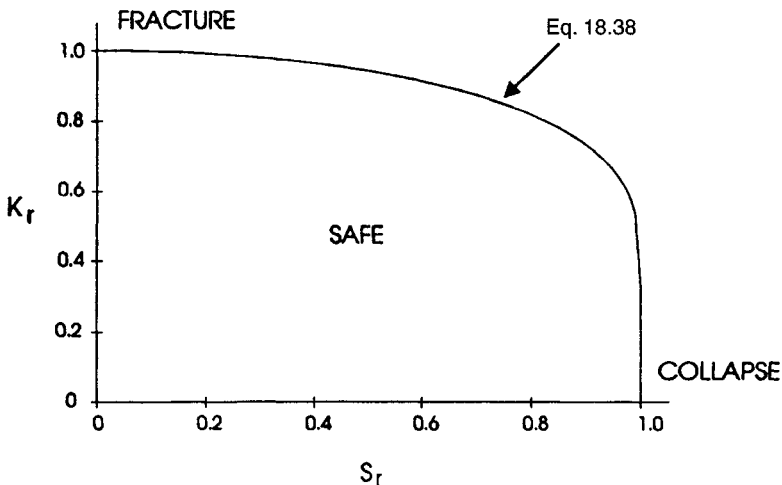


**Fig. 18.13** Failure assessment diagram.